266

Long-Range Forecasting and Climate Research

The relationship between sea surface temperature anomalies and summer rainfall in Africa 4 - 20°N

by

M N Ward, J A Owen, C K Folland and G Farmer

LRFC 32 OCTOBER 1989

Meteorological Office (Met. O. 13)
London Road
Bracknell
Berkshire RG12 2SZ

ORGS UKMO L
National Meteorological Library
FitzRoy Road, Exeter, Devon. EX1 3PB

THE RELATIONSHIP BETWEEN SEA SURFACE TEMPERATURE ANOMALIES AND SUMMER RAINFALL IN AFRICA 4 - 20°N

(LRFC 32)

BY

M N WARD, J A OWEN, C K FOLLAND AND G FARMER *

Proceedings of the commonwealth Meteorologists Conference, Shinfield Park, Reading, June 1989.

LONDON, METEOROLOGICAL OFFICE.
Long-Range Forecasting and Climate Research Memo.LRFC.32

The relationship between sea surface temperature anomalies and summer rainfall in Africa 4-20 deg N.

06790190

551.577.3
551.513.2
551.526.6

MET O 13 (SYNOPTIC CLIMATOLOGY BRANCH)
METEOROLOGICAL OFFICE
LONDON ROAD
BRACKNELL
BERKSHIRE RG12 2SZ

OCTOBER 1989

NB. This paper has not been published. Permission to quote from it should be obtained from the Assistant Director (Synoptic Climatology), Meteorological Office, UK.

* Climatic Research Unit
University of East Anglia
Norwich

3 8078 0001 3077 5

Abstract

In the current century, marked interannual and interdecadal rainfall variability is evident from station rainfall records for sub-Saharan Africa. In summer, anomalous sea surface temperature (SST) patterns both local to and remote from the region are shown to be statistically correlated with seasonal sub-Saharan rainfall, expressed in this paper in standardised units. To support the empirical evidence, a general circulation model (GCM) of the atmosphere is used to model the impact on sub-Saharan rainfall of the observed worldwide SST pattern in 1950, 1958, 1976, 1983, 1984 and 1988; these six years provide a good sample of the different rainfall patterns that can be observed in the study region. The modelled rainfall is close to that observed in the study region in each year, supporting the idea that anomalous patterns of SST can force large-scale rainfall anomalies in the region. Statistical forecast methods and, more tentatively, methods using a GCM are being developed based on the SST anomaly pattern observed prior to the rainfall season.

Introduction

In the last decade, there have been considerable advances in knowledge and understanding of interannual climate variability in the tropics. Theory and observation suggest that, on a seasonal time scale and relative to the atmosphere at middle latitudes, the tropical atmosphere should give a clearer and more direct response to variations in boundary forcing. This paper argues that variations in sea surface temperature patterns have an important influence on seasonal rainfall variations in sub-Saharan Africa. The work reported here follows on from that of Folland, Palmer and Parker (1986).

Observational evidence

The area of sub-Saharan Africa under study is shown in Figure 1. Station rainfall data (when available) have been combined into standardised unit (SU) May-October rainfall anomaly time series for each region in Figure 1. May-October covers the period when seasonal rains associated with the intertropical convergence zone migrate north to the edge of the Sahara desert and then, having left a drier period on the Guinea Coast in August, the rains retreat south again. Earlier work (Folland, Palmer and Parker, 1986) concentrated on the belt covering about 4 degrees of latitude situated to the south of the Sahara desert called the Sahel, for which an SU rainfall series was produced by Nicholson (1985). Nicholson's series gives annual rainfall anomalies, though the July-September peak of the summer rainfall season typically makes up about 90% of the Sahel's annual rainfall.

Sea surface temperature data were taken from the Meteorological Office Historical Sea Surface Temperature dataset (MOHSST) (Parker and Folland, 1988). For the analyses presented here, the data were expressed as 10°x10° seasonal departures (anomalies) from the 1951-80 seasonal normal.

We have calculated unrotated and rotated covariance eigenvectors of the global SST anomaly data. The eigenvectors identify several important patterns of large scale SST anomaly variability (described more fully in Parker and Folland (1989)). The eigenvector coefficient time series trace the history (strength and sign) of the SST anomaly patterns described by the eigenvectors. These time series have been useful in identifying the SST anomaly - rainfall relationships. The clearest relationships are summarised below.

The third (unrotated) covariance eigenvector (Fig 2a) has negative weights in the N Atlantic and N Pacific and positive weights in the S Atlantic and Indian Oceans. The time series of this pattern has a quite strong negative correlation with Nicholson's Sahel series (Fig 2b) suggesting that, when the N Atlantic and N Pacific SST anomalies are higher (lower) than those in the S Atlantic and Indian Ocean, the rainfall across the Sahel is usually above (below) normal. This is found to be true for May-October rainfall over much of the study region (Fig 2c),

except for the near equatorial regions where the link is very weak. Cross spectral analyses confirm the visual impression gained from Figure 2b that this SST anomaly pattern is largely associated with Sahel rainfall variations on a decadal time scale, though shorter time scale fluctuations show some coherence with the SU series, especially before about 1945.

A more localised eigenvector pattern, derived after rotation of eigenvectors 4 to 13, is also related to the SU series. The pattern is mainly confined to the tropical Atlantic, strongest in the Benguela current region of the S Atlantic, with weights of opposite sign in the north Atlantic (Fig 3a, similar to Lough, 1985). The coefficient time series for this eigenvector accounts for an additional fraction of Sahel rainfall variability (Fig 3b). Its association with the SU rainfall series differs in two major respects from that of the eigenvector in Fig 2. Firstly, cross spectral analyses (not shown) indicate strongest coherence with Sahel rainfall on time scales from the interannual to a few years. Secondly, this eigenvector pattern has a quite strong positive correlation with rainfall on the Guinea coast, though the eigenvector pattern is insufficient to describe this SST anomaly - rainfall link very well because rainfall in the Guinea coast region correlates positively with SST anomalies in the Benguela current region and much of the north tropical Atlantic as well (Fig 4). Note also that sub-regions within the Sahel have subtly different links with tropical Atlantic SST anomalies (Fig 4).

A covariance SST anomaly eigenvector coefficient time series representing El Nino and La Nina (the second unrotated eigenvector, not shown) has weak negative correlations with most of the SU rainfall series, suggesting rainfall tends to be lower (higher) in years of El Nino (La Nina) events. The strongest links are in the eastern regions of Fig 1, where correlations with May-October rainfall over 1946-86 are typically about -0.4.

General Circulation Model results

The Met Office general circulation model (GCM) that we have used has 11 levels in the vertical and a horizontal grid with a spacing of 2.5° of latitude and 3.75° of longitude (the model is similar to that described by Cunnington and Rowntree, 1986). We have assessed the ability of the model to simulate the observed Sahel rainfall in six past years when it is forced with the observed worldwide SSTs in those years. For each year chosen, an experiment was carried out which started from the observed atmospheric conditions of 26 March 1984 and which ran for seven months to the end of October. The only difference between these experiments is the imposed SST forcing, which was updated every five days using data for the chosen year from the MOHSST dataset. In data sparse areas, mainly confined to the Southern Ocean, extrapolations were made by combining the limited SST data with climatology. Climatological ice limits were also used.

The difference, averaged over July-Sept, in the observed rainfall rate between 1984 (very dry in the Sahel) and 1950 (very wet in

the Sahel) is shown in Fig 5a. This is similar to the difference simulated by the GCM for the two years (Fig 5b), with 1984 drier across the Sahel and wetter along the Guinea coast, though here the magnitude of the modelled differences is less than the observed. A rainfall anomaly dipole, with substantial anomalies in the Sahel of opposite sign to substantial anomalies near the Guinea coast, has been observed in many years, and was correctly simulated by the GCM in an experiment for 1958, when rainfall was below normal on the Guinea coast and much above normal in the Sahel. The three other years studied with the GCM, 1983 (very dry in the Sahel), 1976 (dry in the Sahel) and 1988 (average in the Sahel) did not have an observed rainfall dipole but were still successfully simulated by the GCM. The first two rows of Table I verify the mean July-September rainfall rate for the Sahel that was simulated by the GCM.

Table I Observed and GCM modelled rainfall over the Sahel.

	YEAR						VERIFICATION	
	1950	1958	1988	1976	1983	1984	r	BIAS
Observed rainfall	5.5	4.2	3.3	2.7	2.0	1.4		
model simulation	5.9	4.7	2.9	2.4	1.3	2.0	0.95	+0.02
mid-July hindcast	5.4	3.7	n/a	3.2	1.6	2.1	0.95	+0.02
June hindcast	6.6	4.1	n/a	2.9	1.4	1.8	0.97	+0.18
May hindcast	4.0	4.2	n/a	4.3	3.1	1.4	0.70	+0.22
April hindcast	3.4	3.3	n/a	3.8	2.4	2.4	0.62	-0.12

Note: Observed and modelled rainfall shown is the mean rainfall rate (mm per day) averaged across the Sahel region (defined in Fig 5a) and averaged over the months July, August and September.
Observed rainfall is estimated using station rainfall data interpolated over the Sahel region defined in Fig 5a.
n/a = not yet available.
VERIFICATION: r = correlation between observed rainfall and modelled values (6 pairs of values for the simulations, 5 for the hindcasts); BIAS = mean modelled rainfall rate minus mean observed rainfall rate.

The mechanisms by which the SSTs effect the rainfall changes in the model are being investigated. One aspect seems to be a change in the flux of moisture into N tropical Africa in the lower troposphere (Fig 6). A problem in isolating the mechanisms is that SSTAs in each of the major ocean basins show some ability to simulate the observed rainfall anomaly in the Sahel. This has been shown by experiments where the observed SSTs were used in part of the world's oceans (eg tropical Pacific), and climatological SSTs were used elsewhere (Table II, also see Folland, Owen and Maskell (1989), and earlier work by Palmer (1986)). Further experiments have shown that the initial atmospheric conditions at the start of the experiment in March are relatively unimportant for the simulated rainfall, and that feedback between the model's soil moisture and the model's atmosphere does not have a large impact on our results. However, insufficient work has been done to determine the relative importance of the latter process in all conditions.

Table II Skill of GCM simulations forced by different ocean areas.

Ocean region	r_a
Globe	0.70
Tropical Atlantic	0.35
Tropical Indian	0.32
Tropical Pacific	0.45
Tropics	0.55
Extratropics	0.23

Notes:
Observed SSTs were used in the given ocean region, climatological SSTs elsewhere.
For each ocean region, experiments were carried out for 1950, 1958, 1983 and 1984. r_a (anomaly correlation between modelled and observed rainfall) was calculated by comparing the modelled monthly rainfall anomaly averaged across the Sahel (defined in Fig 5a) with the observed monthly rainfall anomaly for each month June through October (so each correlation is based on 5 months x 4 years = 20 pairs of modelled and observed anomalies).

Seasonal Sahel rainfall prediction based on sea surface temperatures

Large scale SST anomaly patterns do not usually change very much over a few months, suggesting that the pre-rainfall season SST anomaly pattern may bring a degree of predictability to sub-Saharan seasonal rainfall. Methods of prediction are being developed based on statistical relationships and, more tentatively, using the GCM. Up to now, prediction for the Sahel as a whole has been most closely investigated. To demonstrate the skill that is currently achieved using statistical methods, Fig 7 (based on Owen and Ward, 1989) shows predictions made using a multiple regression of Nicholson's Sahel SU rainfall series on time series values similar to those in Figs 2b and 3b, but using March-April SST anomalies. The forecasts have skill both before 1945, when interannual variability dominates, and after 1945, when there is considerable interdecadal variability as well.

To use the GCM for prediction, an estimate of the SSTs during the rainfall season must be given to the model. The simplest method is to assume that the SST anomalies at the time of the forecast remain constant, and to create SST fields by adding these anomalies to the varying SST climatology through the coming prediction period. Table I summarises the success of 'hindcasts' made using SST anomalies for various lead times on the Sahel rainfall season. Hindcasts from June and mid-July SST anomalies show similar skill to the simulations which used the observed SST, but the hindcast skill becomes small when April SST anomalies are used. The inference from this limited number of prediction experiments is that this GCM method may provide useful seasonal predictions for July to September rainfall based on June SST anomalies (ie forecast run in early July), but that for longer lead times, persistence of the SST anomalies is insufficient to provide an adequately accurate summer SST field.

Experimental Forecasts

Seasonal rainfall forecasting may become possible for a number of tropical regions based on SST anomalies observed prior to the rainfall season. Experimental forecasts for the Sahel and the drought-prone region of NE Brazil have been produced in real-time for each rainfall season since the 1986 Sahel and 1987 NE Brazil rainfall seasons. The three NE Brazil forecasts and the first two Sahel forecasts all showed clear skill (Owen and Ward (1989), Ward and Folland (1989)). The Sahel forecasts for 1988 and 1989 in Fig 7 show that in these years the predictive statistical relationships performed poorly. Also shown in Fig 7 is the result for 1988 and 1989 of a similar multiple regression but using August SST anomalies. These estimates are much less in error showing that part of the problem has been unusually rapid changes in the SSTA pattern from the time of the forecast to the rainfall season. However, even from August SST anomalies, the estimated rainfall is less than the observed, suggesting better SST predictors are needed, or factors other than SST should be considered, or that there may be a bias in some of the recent SST data. We are considering all of these possibilities. It is also necessary to study the considerable large-scale spatial variation that sometimes occurs in the seasonal rainfall anomaly across the Sahel. Progress in this has been briefly mentioned (eg Fig 4a-b), and its importance has been underlined by rainfall in 1989: January-September rainfall has been above the 1951-80 normal at 7 out of the 12 stations reporting from the western third of the Sahel (stations west of 2°W that we use for our annual SU series), but in the rest of the Sahel, only 2 out of 15 stations have reported above normal rainfall, with many reporting less than 80% of normal.

A number of GCM predictions were made for 1989, and these will be discussed elsewhere.

Conclusions

Patterns of sea surface temperature anomalies in different parts of the global ocean seem to strongly influence seasonal rainfall in tropical North Africa. Empirical links over much of this century between SST anomalies and seasonal sub-Saharan rainfall have been explored using eigenvectors of SST anomalies, but additional statistical approaches are needed to better identify the nature of these links.

The general circulation model used here is capable of simulating the main features of the observed summer rainfall anomaly pattern in the Sahel and W Africa in all six years studied. The years studied included very dry, average and very wet years in the Sahel. Contributions to the skilful simulations appear to derive from SST anomalies in all ocean basins. Though worldwide tropical SST anomalies are the most important, extratropical anomalies probably play some role.

References

Cunnington, W.M. and Rowntree, P.R. 1986. Simulations of the Saharan atmosphere - dependence on moisture and albedo, Quart. J. R. Met. Soc., 112, 971-999.

Folland, C.K., Palmer, T.N. and Parker, D.E. 1986. Sahel rainfall and worldwide sea temperatures, 1901-85, Nature, 320, 602-607.

Folland, C.K., Owen, J.A. and Maskell K. 1989. Physical causes and predictability of variations in seasonal rainfall over sub-Saharan Africa, in: Remote Sensing and large-scale global processes, IAHS Publ. no. 186, 87-95.

Lough, J.M. 1986. Tropical Atlantic sea surface temperatures and rainfall variations in Subsaharan Africa, Mon. Weath. Rev., 114, 561-570.

Nicholson, S.E. 1985. Sub-Saharan rainfall 1981-1984, J. Clim. Appl. Met., 24, 1388-1391.

Owen, J.A. and Ward, M.N. 1989. Forecasting Sahel rainfall, Weather, 44, 57-64.

Palmer, T.N. 1986. Influence of the Atlantic, Pacific and Indian Oceans on Sahel rainfall, Nature, 322, 251-253.

Parker, D.E. and Folland, C.K. 1988. 'The Meteorological Office Historical Sea Surface Temperature Dataset', In: Recent Climatic Change - a regional approach. Ed S. Gregory, Belhaven Press, 41-50.

Parker, D.E. and Folland, C.K. Worldwide surface temperature trends since the mid-19th Century, in: Proc. U.S. D.o.E. Workshop on Greenhouse-Gas-Induced Climatic Change, Amherst, Mass., May 1989, Elsevier (in press)

Ward, M.N. and Folland, C.K. 1989. Statistical prediction of NE Brazil seasonal rainfall from sea surface temperatures. LRFC31 (internal publication, available from the Meteorological Office). Submitted to International Journal of Climatology.

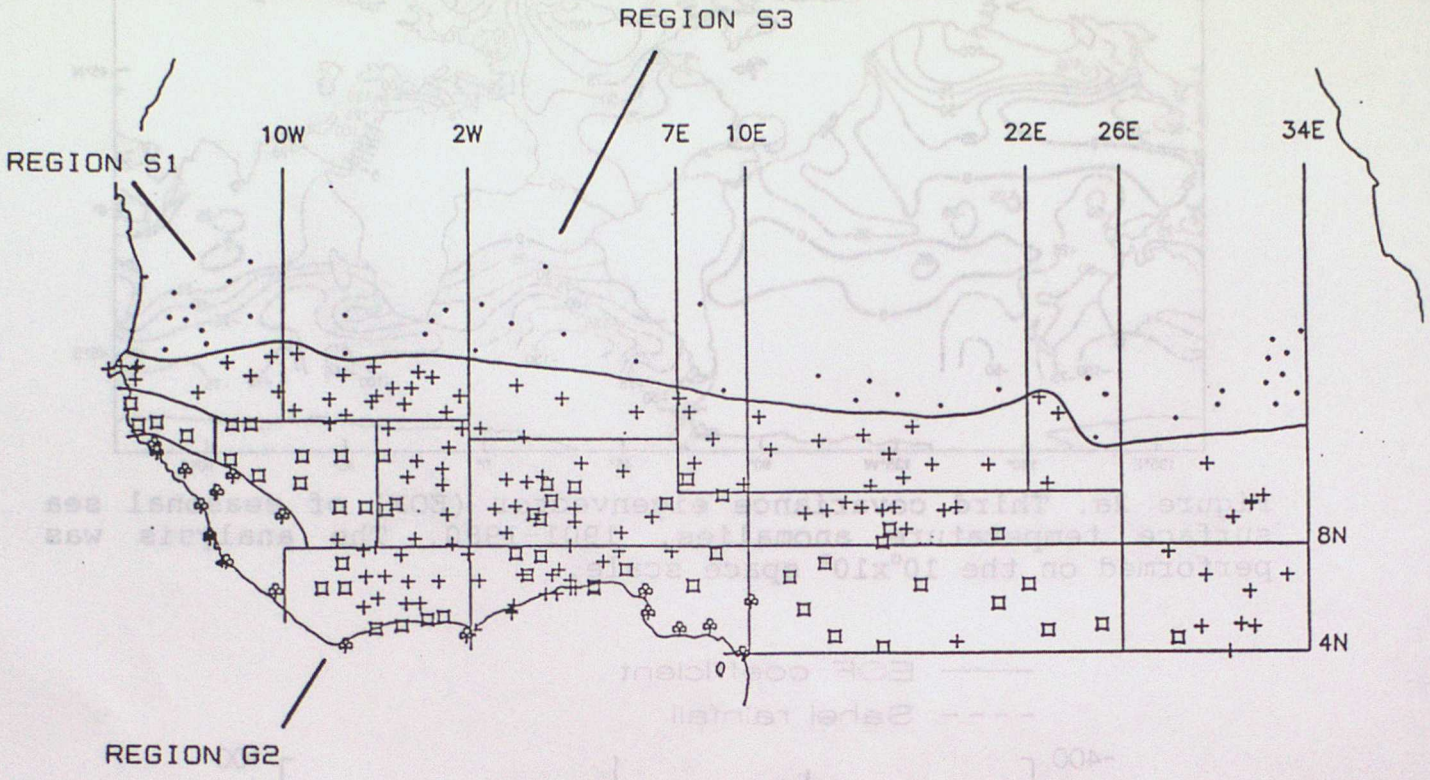

Figure 1. Rainfall stations used so far in the statistical analyses. Symbols indicate the mean May to October rainfall for that station:

- • = 100 to 500 mm
- + = 500 to 1100 mm
- ⌑ = 1100 to 1600 mm
- ⌖ = >1600 mm

The belt of stations with a mean rainfall of 100-500mm marks the approximate region that Nicholson defined as the Sahel. Standardised 1946-1986 time series of the total May to October rainfall anomaly have been produced for each of the 24 regions.

The regions S1, S3, and G2 are used for Figure 4.

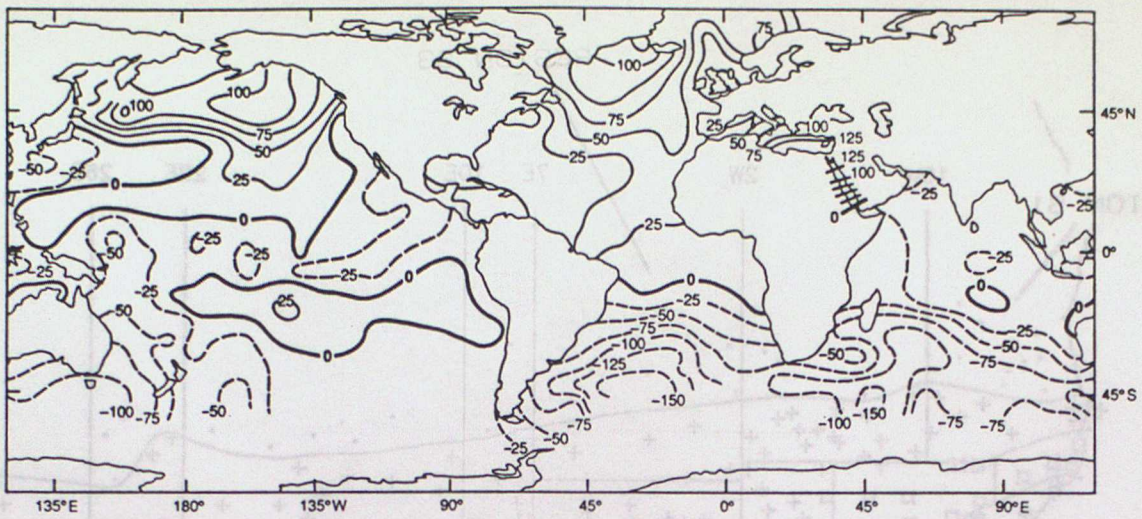

Figure 2a. Third covariance eigenvector (EOF) of seasonal sea surface temperature anomalies, 1901-1980. The analysis was performed on the 10°x10° space scale.

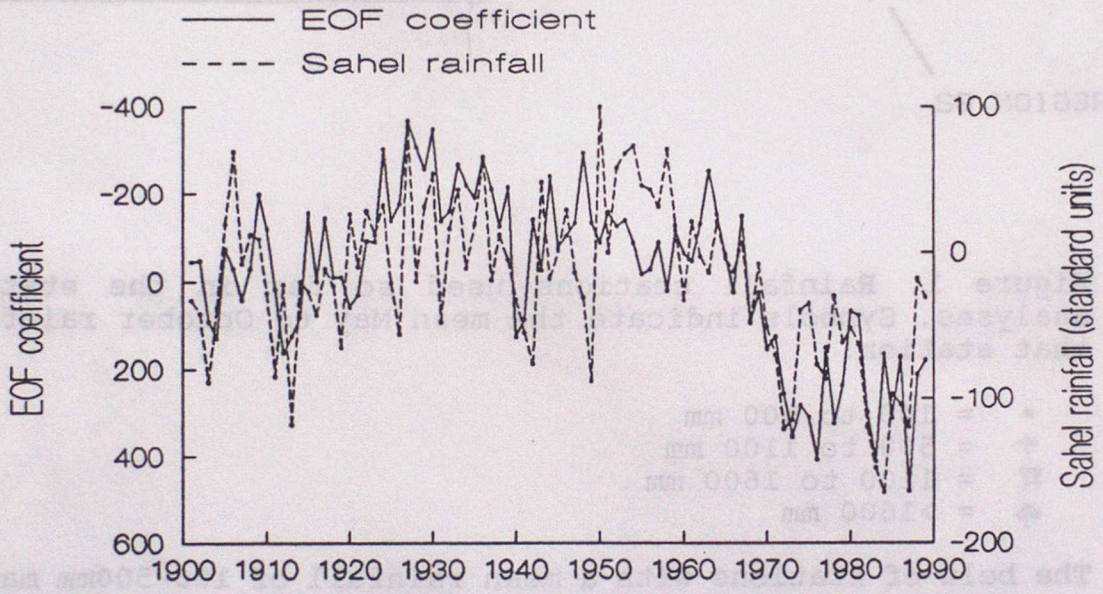

Figure 2b. Coefficient time series of the above EOF (values for July-Sept) and annual Sahel rainfall, 1901-1989. Rainfall values to 1984 are from Nicholson, values after 1984 are based on CLIMAT reports; 1989 is a preliminary estimate based on data to the end of September. Correlation between the two series is -0.63.

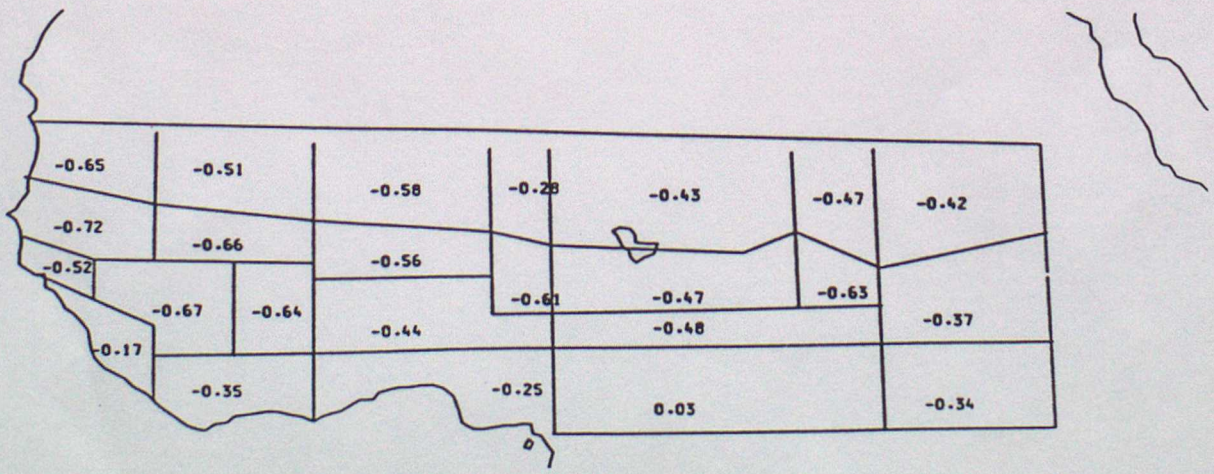

Figure 2c. 1946-1986 correlation between May-October rainfall time series for given box and coefficient time series of the above EOF (values for May-October).

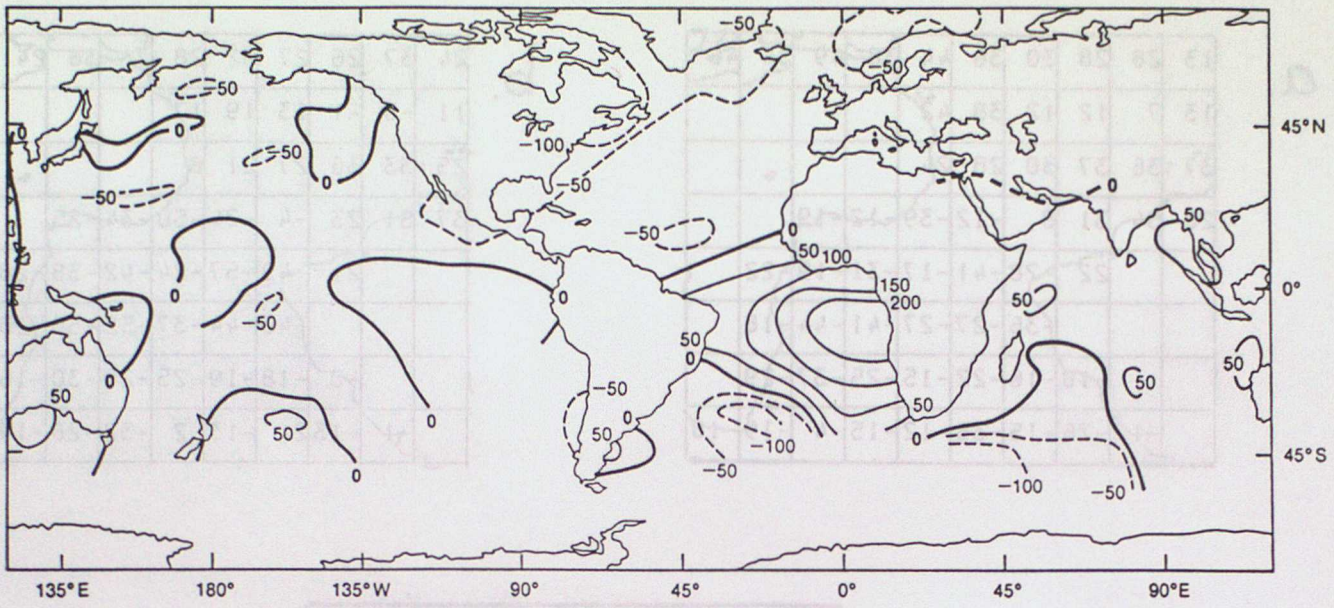

Figure 3a. VARIMAX rotated EOF of seasonal sea surface temperature anomalies, 1901-1980. EOFs 4 to 13 were rotated and this is the second of those solutions.

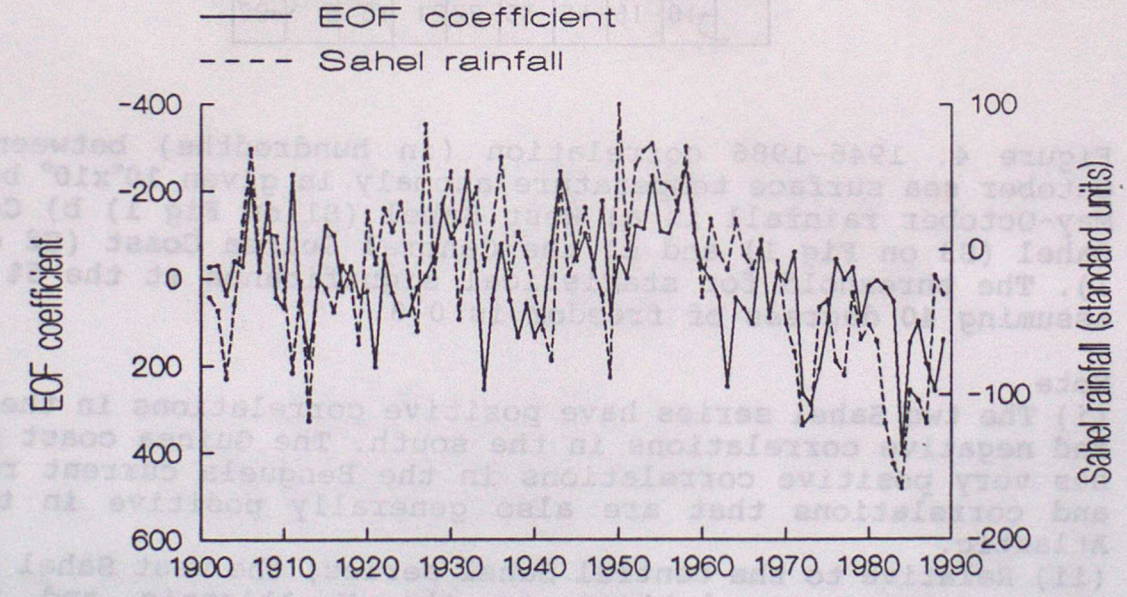

Figure 3b. Coefficient time series of the above EOF (values for July-Sept) and annual Sahel rainfall, 1901-1989. Correlation between the two series is -0.51.

a.

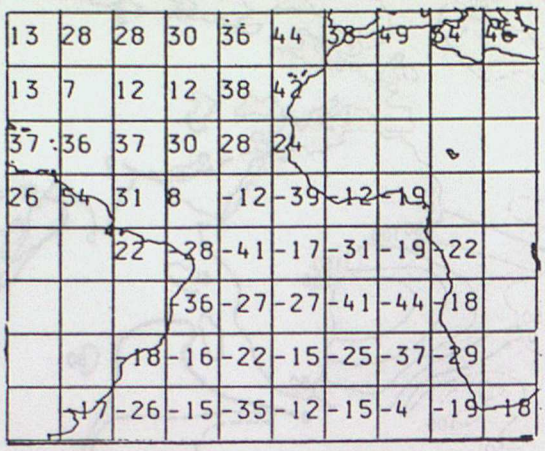

b.

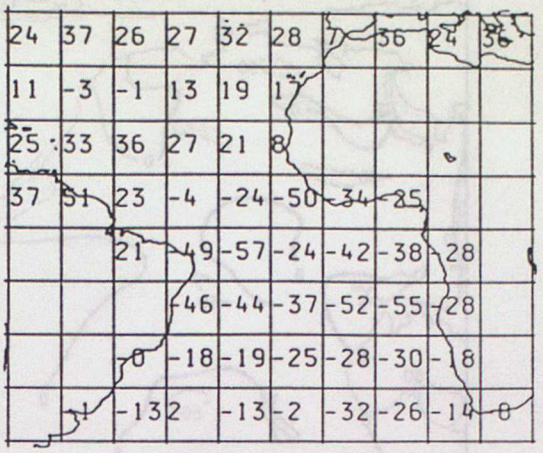

c.

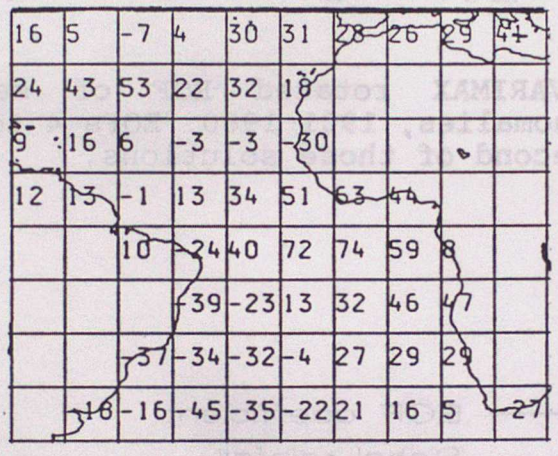

Figure 4. 1946-1986 correlation (in hundredths) between May-October sea surface temperature anomaly in given 10°x10° box and May-October rainfall in a) West Sahel (S1 on Fig 1) b) Central Sahel (S3 on Fig 1) and c) the Central Guinea Coast (G2 on Fig 1). The threshold for statistical significance at the 5% level assuming 40 degrees of freedom is 0.3.

Note
(i) The two Sahel series have positive correlations in the north and negative correlations in the south. The Guinea coast series has very positive correlations in the Benguela current region, and correlations that are also generally positive in the N Atlantic.
(ii) Relative to the central Sahel series, the west Sahel series has stronger correlations in the N Atlantic and weaker correlations in the S Atlantic.

a.

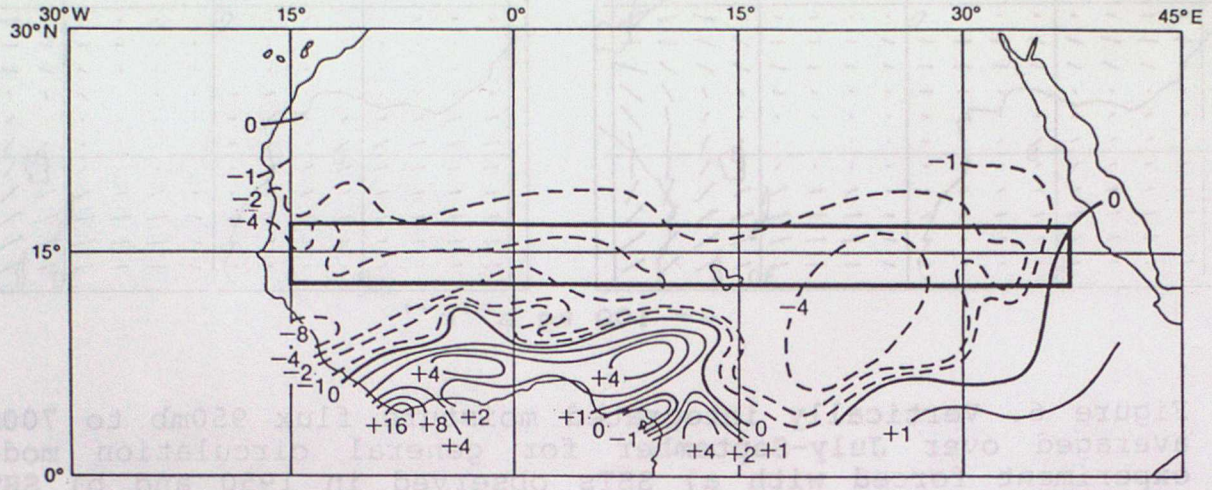

b.

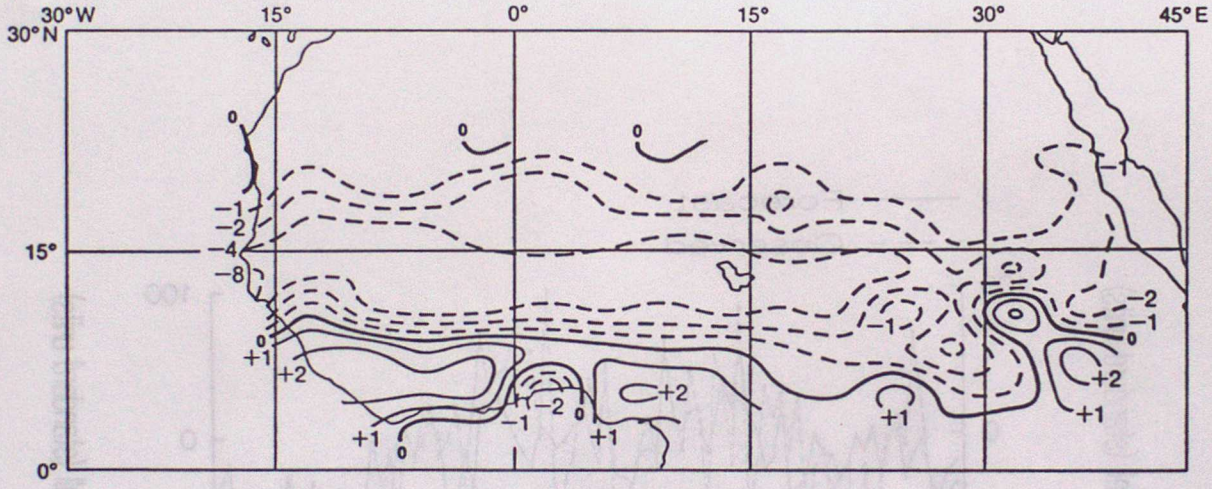

Figure 5. 1984 minus 1950 rainfall rate (mm per day) averaged over July to September: a) observed b) simulated by the general circulation model in experiments using the observed SST to force the model. The solid box marked on a) indicates the region defined as the Sahel for model verification in Tables I and II.

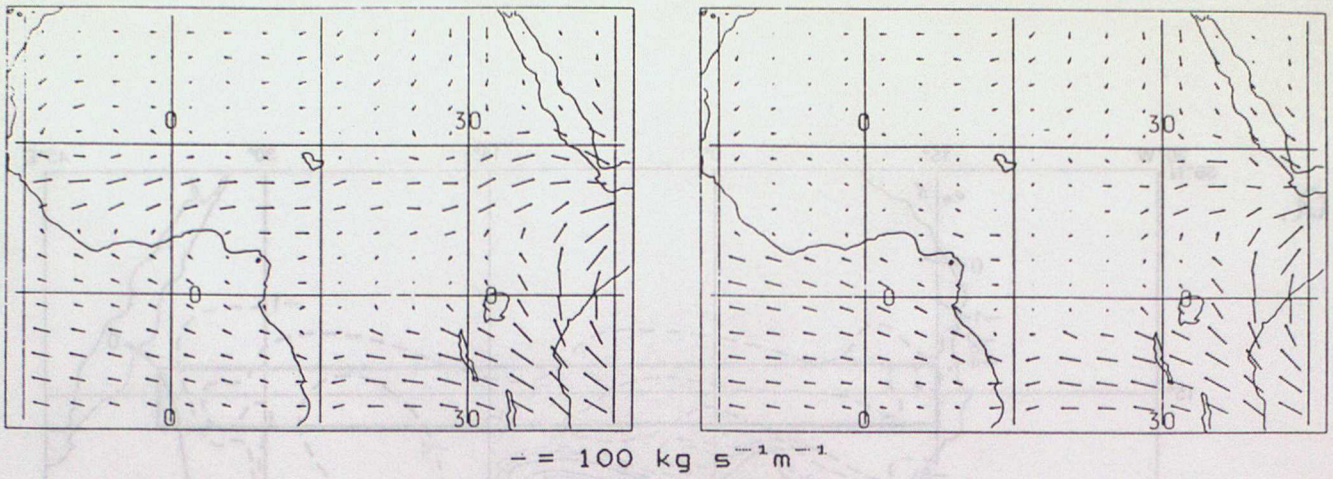

Figure 6. Vertically integrated moisture flux 950mb to 700mb averaged over July-September for general circulation model experiment forced with a) SSTs observed in 1950 and b) SSTs observed in 1984.

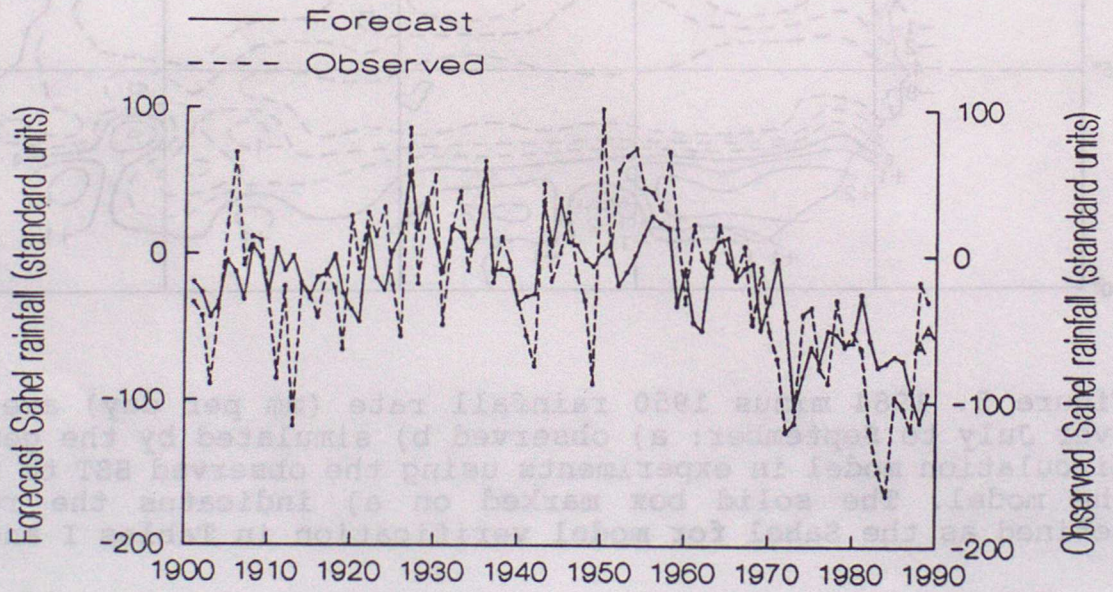

Figure 7. Forecasts of annual Sahel rainfall for each year from 1901 to 1989 made using a multiple regression statistical model. Forecasts are made from March-April time series vales of the eigenvector patterns in Figs 2a and 3a. The points for 1988 and 1989 marked with the letter 'A' indicate expected rainfall from a multiple regression using August values of the eigenvector time series. The dashed line is the observed Sahel rainfall. Forecasts for 1901-1945 (correlation with observed = 0.52) are made using 1946-1988 model parameters, and 1946-1989 forecasts (correlation with observed = 0.63) use 1901-1945 model parameters.

INDEX TO LONG-RANGE FORECASTING AND CLIMATE RESEARCH SERIES

1) THE CLIMATE OF THE WORLD - Introduction and description of world climate.
by C K Folland (March 1986)

2) THE CLIMATE OF THE WORLD - Forcing and feedback processess.
by C K Folland (March 1986)

3) THE CLIMATE OF THE WORLD - El Nino/Southern Oscillation and the Quasi-biennial Oscillation.
by C K Folland (March 1986)

4) THE CLIMATE OF THE WORLD - Climate change: the ancient earth to the 'Little Ice Age'.
by C K Folland

5) THE CLIMATE OF THE WORLD - Climate change: the instumental period.
by C K Folland (March 1986)

6) THE CLIMATE OF THE WORLD - Carbon dioxide and climate (with appendix on simple climate models).
by C K Folland (March 1986)

7a) Sahel rainfall, Northern Hempishere circulation anomalies and worldwide sea temperature changes, (To be published in the Proceedings of the "Pontifical Academy of Sciences Study Week", Vatican, 23-27 September 1986).
by C K Folland, D E Parker, M N Ward and A W Colman (September 1986) (Amended July 1987)

8) Lagged-average forecast experiments with a 5-level general circulation model.
by J M Murphy (March 1986)

9) Statistical Aspects of Ensemble Forecasts.
by J M Murphy (July 1986)

10) The impact of El Nino on an Ensemble of Extended-Range Forecasts. (Submitted to Monthly Weather Review)
by J A Owen and T N Palmer (December 1986)

11) An experimental forecast of the 1987 rainfall in the Northern Nordeste region of Brazil.
by M N Ward, S Brooks and C K Folland (March 1987)

12) The sensitivity of Estimates of Trends of Global and Hemispheric Marine Temperature to Limitations in Geographical Coverage.
by D E Parker (April 1987)

13) General circulation model simulations using cloud distributions from the GAPOD satellite data archive and other sources.
by R Swinbank (May 1987)

14) Similation of the Madden and Julian Oscillation in GCM Experiments.
by R Swinbank (May 1987)

15) Numerical simulation of seasonal Sahel rainfall in four past years using observed sea surface temperatures.
by J A Owen, C K Folland and M Bottomley (April 1988)

16) Not used

17) A note on the use of Voluntary Observing Fleet Data to estimate air-sea fluxes.
by D E Parker (April 1988)

18) Extended-range prediction experiments using an 11-level GCM
by J M Murphy and A Dickinson (April 1988)

19) Numerical models of the Raingauge Exposure problems - field experiments and an improved collector design.
by C K Folland (May 1988)

20) An interim analysis of the leading covariance eigenvectors of worldwide sea surface temperature anomalies for 1901-80.
by C K Folland and A Colman (April 1988)

21) Prospects for long range forecasting for the United Kingdom.
by A Dickinson and C K Folland (July 1988)

22) CLIMATE OF THE WORLD (Restricted Issue)
1. Introduction to world climate
2. Description of world climate
by C K Folland and D E Parker (July 1988)

23) CLIMATE OF THE WORLD (Restricted issue)
3. Climatic forcing and feedback processes.
I. Forcing from above.

4. Climatic forcing and feedback processes.
II. Interactions with land surface
by C K Folland and D E Parker (July 1988)

24) CLIMATE OF THE WORLD (Restricted Issue)
5. Ocean-atmosphere interaction
by D E Parker and C K Folland (July 1988)

25) CLIMATE OF THE WORLD (Restricted Issue)
6. The El Nino/Southern Oscillation, the Quasi-Biennial Oscillation, and the 30-60 day variations.
by C K Folland and D E Parker (July 1988)

26) CLIMATE OF THE WORLD (Restricted Issue)
7. A review of palaeoclimate from the early Earth to the Pleistocene ice ages

8. Climate from the late glacial to the "Little ice age"
by C K Folland and D E Parker (July 1988)

27) CLIMATE OF THE WORLD 9. (Restricted issue) — Climatic change in the instrumental period by D E Parker and C K Folland (July 1988)

28) CLIMATE OF THE WORLD 10. (Restricted issue) — Carbon dioxide and other greenhouse gases, and climatic variation (with appendix on simple climate models). by D E Parker and C K Folland (July 1988)

29) Comparison of corrected sea surface and air temperature for the globe and the hemispheres 1856-1988 - Presented at the 12th Annual Climate Diagnostics Workshop. Boston, USA, 30 Oct - 4 Nov 1988.
by C K Folland and D E Parker (November 1988)

30) Development of a Sahel rainfall series using CLIMAT data
by A W Colman (December 1988)

31) Statistical prediction of North East Brazil seasonal rainfall from SSTs
by M N Ward and C K Folland (September 1989)

32) The relationship between SST anomalies and summer rainfall in Africa 5-20° North (provisionally)
by M N Ward, J A Owen, C K Folland & G Farmer (CRU)
(October 1989)